Journal of Physical and Theoretical Chemistry
of Islamic Azad University of Iran, 13 (2) 155-171: Summer 2016
(J. Phys. Theor. Chem. IAU Iran)
ISSN 1735-2126

Theoretical investigations on molecular structure, NBO, HOMO-LUMO and MEP analysis of two crystal structures of *N*-(2-benzoyl-phenyl) oxalyl: A DFT study

Masoome Sheikhi[a,*], Ebrahim Balali[b] and Hadi Lari[c]

[a] Young Researchers and Elite Club, Gorgan Branch, Islamic Azad University, Gorgan, Iran
[b] Department of Pharmaceutical Chemistry, Faculty of Pharmaceutical Chemistry, Pharmaceutical Sciences Branch, Islamic Azad University, Tehran, Iran
[c] Department of Chemistry, Mashhad Branch, Islamic Azad University, Mashhad, Iran

Received April 2016; Accepted July 2016

ABSTRACT

The *N*-(2-benzoyl-phenyl) oxalyl derivatives are important models for studying of three-centered intramolecular hydrogen bonding in organic molecules. The quantum theoretical calculations for two crystal structures of *N*-(2-benzoyl-phenyl) oxalyl (compounds **I** and **II**) were performed by Density Functional Theory (B3LYP method and 6-311+G***** basis set). From the optimized structures, geometric parameters were obtained and experimental measurements were compared with the calculated data. The NMR parameters such as chemical shift isotropic (CS^I) and chemical shift anisotropic (CS^A), natural charge (NBO), thermodynamic parameters such as relative energy (ΔE), standard enthalpies (ΔH), entropies (ΔS), Gibbs free energy (ΔG) and constant volume molar heat capacity (Cv), frontier molecular orbitals (FMOs), total density of states (DOS), molecular electrostatic potential (MEP) of the two structures were investigated by theoretical calculations. Molecular properties such as Ionisation Potential (*I*), Electron affinity (*A*), chemical hardness (η), electronic chemical potential (μ) andelectrophilicity (ω) obtained and three-centered intramolecular hydrogen bonding were investigated by NBO analysis.

Keywords: oxalyl; DFT; DOS; Natural charge; NBO analysis

INTRODUCTION

Oxamide derivatives are used as a model to study bonds in biomolecules, particularly intermolecular and intramolecular hydrogen bonding [1]. The hydrogen bond is a weak chemical bond between an electronegative atom, such as fluorine, oxygen or nitrogen and a hydrogen atom bound to another electronegative atom. Hydrogen bonds are responsible of water and many biological molecules [2-4]. These hydrogen-bond attractions can occur between molecules (intermolecular) or within different parts of a single molecule (intramolecular) [5]. A three-center intramolecular hydrogen bonding interaction can be seen in all oxamides. Three-center intramolecular hydrogen bonding is bifurcated hydrogen bonding. There are two types of bifurcated hydrogen bonding in biological systems, organic compounds, that can be as intermolecular, intramolecular or both. One is three centered hydrogen bond where a electronegative atom participate as

[*]Corresponding author: m.sheikhi@gorganiau.ac.ir

acceptor group and two hydrogen atoms as donor in two different hydrogen bonds, and the other kind is where two same electronegative atoms participate as acceptor groups and a hydrogen as acceptor atom [6].

In recent years, computational chemistry has become an important tool for chemists and a well-accepted partner for experimental chemistry [7-10]. Density functional theory (DFT) method has become a major tool in the methodological arsenal of computational organic chemists [11]. Isabel Rozas and et al. investigated bifurcated or three-centered hydrogen bonds (HB) using DFT (B3LYP/6-31G*) on different families of compounds such as monomers with intramolecular three-centered HB, dimers with a HB donor (HBD) and a molecule with two HB acceptor (HBA) groups, and trimers with one HBD and two HBAs [12]. A. Lakshmipriya et al. studied existence of three-centered C=O…H(N)…X-C hydrogen bond in diphenyloxamide derivatives involving halogens using NMR spectroscopy and quantum theoretical studies [13]. Martinez-Martinez reported synthesis of *N*-(2-benzoyl-phenyl) oxalyl derivatives [14]. Three crystal structures *N*-(2-benzoylphenyl) acetamide, *N*-(2-benzoylphenyl) oxalamate and *N1*,*N2*-bis(2-benzoylphenyl)oxalamide is reported by Carlos Z. Gomez-Castro et al [15]. They studied the formation of three-center hydrogen bonds in three oxalyl derivatives was by the X-ray diffraction analysis. In the present work, we investigate the energetic and structural properties of title two crystal structures (*N*-(2-benzoylphenyl) oxalamate and *N1*, *N2*-bis(2-benzoylphenyl)oxalamide) using DFT calculations. The optimized geometry, frontier molecular orbitals (FMO), detail of quantum molecular descriptors, molecular electrostatic potential (MEP), chemical tensors, natural charge and three-center hydrogen bonds using NBO analysis were calculated.

COMPUTATIONAL METHODS

In this work, we have carried out quantum theoretical calculations for the compounds **I** and **II** using B3LYP/6-311+G* level (DFT) [16] by the Gaussian 03W program package [17] and calculate their properties. At first we have optimized structure using Gaussian 03W program (see Figure 1). We calculated NMR parameters such as chemical shift isotropic (CS^I) and chemical shift anisotropic (CS^A) for title structuresusing B3LYP/6-311+G* level [18,19]. The electronic properties such as E_{HOMO}, E_{LUMO}, HOMO-LUMO energy gap (ΔE), E_{HOMO-1}, E_{LUMO+1}, natural charges, molecular properties, dipole moment (μ_D) and point group were detected [20]. The optimized molecular structure, HOMO and LUMO surfaces were visualized using GaussView 03 program [21]. We also studied the thermodynamic parameters of molecules using the B3LYP/6-311+G* level, and obtained the energy (ΔE), enthalpies (ΔH), Gibbs free energy (ΔG), entropiy (S) and constant volume molar heat capacity (Cv) of the structures [20,22]. The electronic structure of compounds **I** and **II** were studied by using Natural Bond Orbital (NBO) analysis at the same level in order to understand various second-order interactions between the filled orbitals of one subsystem and vacant orbitals of another subsystem, which is a measure of the inter-molecular delocalization or hyper conjugation [18]. We also is obtained the calculated natural charge (NBO) of three structures.

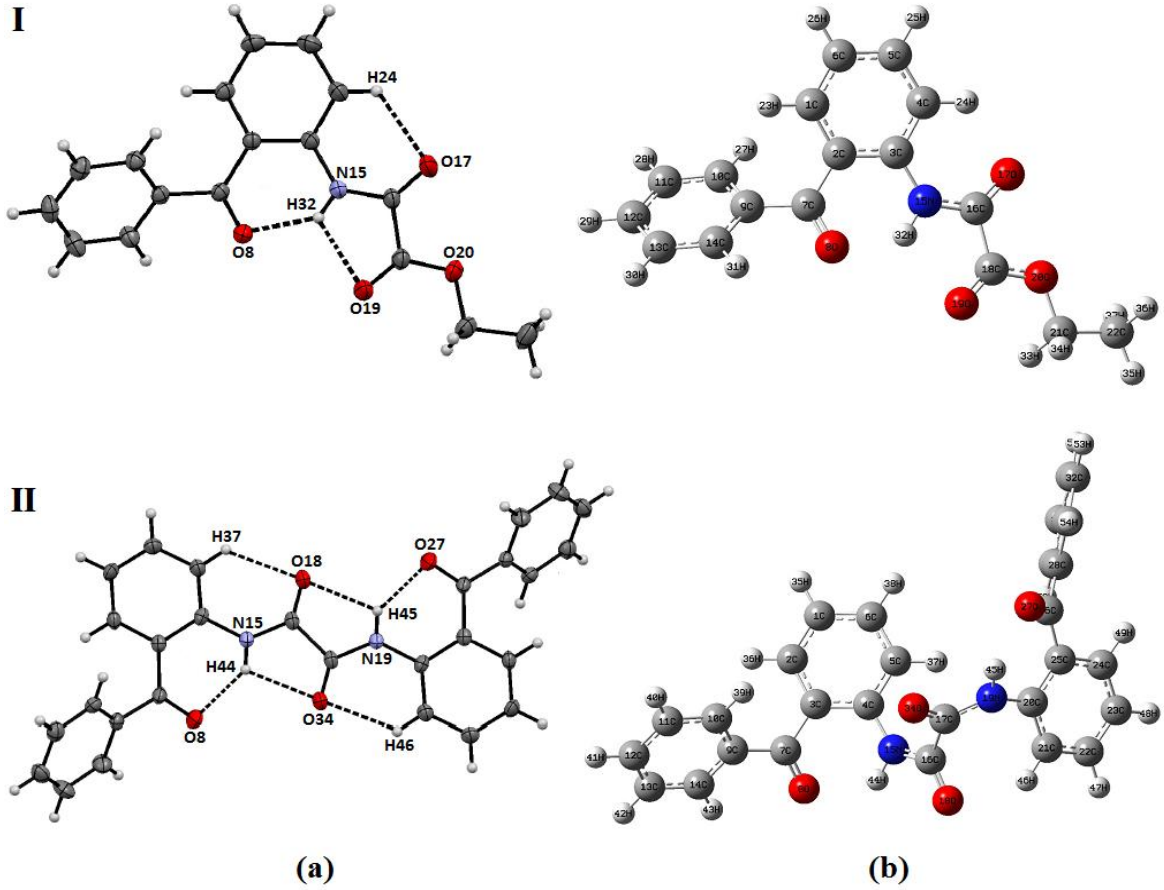

Fig. 1. (a) The Crystallographic numbering of the compounds **I** and **II**, (b) The theoretical geometric structure of the compounds **I** and **II** (optimized with B3LYP/6-311+G* level).

RESULTS AND DISCUSSION

Optimized geometry

The optimized structure of the molecules **I** and **II** has been calculated by DFT (B3LYP/6-311+G*) (see Figure 1) and the selected bond lengths and bond angles of the crystallographic structures[15] and the theoretical parameters of listed in Table 1. As can be seen in Table 1, the calculated parameters show good approximation and can be used as a foundation to calculate the other parameters for the title compounds. We found that most of the calculated bond lengths are slightly longer than X-ray values that it is due to the fact that experimental result corresponds to interacting molecules in the crystal lattice, whereas computational method deals with an isolated molecule in gaseous phase [23,24]. The average differences of the theoretical parameters from the experimental for bond lengths of compound **I** were found to be about 0.01Å (O_{17}-C_{16}), 0.001Å (O_8-C_7), 0.003Å (N_{15}-C_3), 0.02Å (N_{15}-C_{16}), 0.008Å (C_3-C_2), 0.006Å (C_2-C_7), 0.012Å (C_{16}-C_{18}), 0.004Å (C_7-C_9). According to Table 1, the bond length of N_{15}-C_3 in X-ray and optimized structure of compound **I** is 1.399Å and 1.402Å respectively, whereas experimental and theoretical value for the bond length of N_{15}-C_{16} is 1.346Å and 1.366Å, respectively. It shown the bond length of N_{15}-C_{16} is shorter than N_{15}-C_3 that it is due

to the fact that lone pair of N_{15} conjugated with the C_{16} (carbonyl group). Also according to Table 1, the average differences of the theoretical parameters from the experimental for bond lengths of compound **II** were found to be about 0.006Å (O_{34}-C_{17}), 0.004Å (O_8-C_7), 0.008Å (N_{15}-C_4), 0.018Å (N_{15}-C_{16}), 0.01Å (C_4-C_3), 0.012Å (C_3-C_7), 0.009Å (C_{16}-C_{17}), 0Å (C_7-C_9). As seen in Table 1, the bond length of N_{15}-C_4 in X-ray and optimized structure of compound **II** is 1.402Å and 1.410Å respectively, whereas experimental and theoretical value for the bond length of N_{15}-C_{16} is 1.350Å and 1.368Å, respectively. It shown the bond length of N_{15}-C_{16} is shorter than N_{15}-C_3 that it is due to the fact that lone pair of N_{15} conjugated with the C_{16} (carbonyl group).

Table 1. Selected bond lengths (Å) of the compounds **I** and **II** (atom labeling according to Fig. 1)

		Exp.[a]	Cal.[b]
I	O_{17}-C_{16}	1.204(3)	1.214
	O_8-C_7	1.227(2)	1.228
	N_{15}-C_3	1.399(2)	1.402
	N_{15}-C_{16}	1.346(2)	1.366
	C_3-C_2	1.416(3)	1.425
	C_2-C_7	1.486(2)	1.492
	C_{16}-C_{18}	1.538(3)	1.550
	C_7-C_9	1.496(2)	1.500
II	O_{34}-C_{17}	1.211(4)	1.217
	O_8-C_7	1.223(5)	1.227
	N_{15}-C_4	1.402(4)	1.410
	N_{15}-C_{16}	1.350(4)	1.368
	C_4-C_3	1.407(4)	1.417
	C_3-C_7	1.483(5)	1.495
	C_{16}-C_{17}	1.548(5)	1.539
	C_7-C_9	1.495(5)	1.495

[a] Taken from Ref. [15].
[b] Calculated using DFT method (B3LYP/6-311+G*)

In addition, the hydrogen bonds length values of experimental [15] and theoretical compounds **I** and **II** summarized in Table 3. X-ray diffraction analysis of compound reveals that the structure is stabilized by intramolecular hydrogen bonding. According to experimental results is obtained by Carlos Z. Gómez-Castro, it revealed compound **I** has three intramolecular hydrogen bonding (see Figure 1) [15]. By knowing the bond length, the strength of the hydrogen bond can be determined as very strong (below 2.5Å), strong (2.5-2.7Å), normal (2.7-2.9Å) and weak (above 2.9Å). The first intramolecular hydrogen bonding of compound **I** [N_{15}-H_{32}…O_{19}], the experimental and theoretical values of bond length H_{32}…O_{19} are 2.25Å and 2.23Å respectively, that suggesting the existence of very strong intramolecular hydrogen bond. In second intramolecular hydrogen bonding of compound **I** [N_{15}-H_{32}…O_8], the experimental bond length H_{32}…O_8 is 1.97Å and calculated value is 1.90Å. This suggesting the intramolecular hydrogen bond N_{15}-H_{32}…O_8 is very strong. In intramolecular three-centered hydrogen bond of O_{19}…H_{32}…O_8, the O_{19}…H_{32} is weaker rather than H_{25}…O_8. The experimental and theoretical values of bond H_{24}…O_{17} [C_4-H_{24}…O_{17}] is good evident for existence third intramolecular hydrogen bonding in structure **I**. According to Figure 1, there are two intramolecular three-centered hydrogen bonds [O_8…H_{44}…O_{34} and O_{18}…H_{45}…O_{27}] in the theoretical geometric structure of **II**. The experimental and theoretical values for bond length of H_{44}…O_{34} are 2.23Å and 3.84Å, respectively. As shown, the theoretical bond length of H_{44}…O_{34} has which suggesting the existence of intramolecular hydrogen bond. The difference of the theoretical value from the experimental for intramolecular hydrogen bond length of H_{44}…O_{34} [N_{15}-H_{44}…O_{34}] in compound **II** was found to be about 1.61Å. While the experimental and calculated

Table 2. Hydrogen-Bond Geometry (Å) (Exp.[a] and Cal.[b]) of compound **I** and **II**

	D-H…A	D-H (Å)		H…A(Å)		D…A(Å)	
		Exp.	Cal.	Exp.	Cal.	Exp.	Cal.
II	N15-H32…O19	0.86	1.02	2.25	2.23	2.666(2)	2.702
	N15-H32…O8	0.86	1.02	1.97	1.90	2.662(2)	2.703
	C4-H24…O17	0.93	1.08	2.29	2.18	2.908(3)	2.889
III	N15-H44…O34	0.86	1.02	2.23	3.84	2.665(4)	3.37
	N15-H44…O8	0.86	1.02	1.98	2.01	2.673(4)	2.742

a Taken from Ref. [15].
b Calculated using DFT method (B3LYP/6-311+G*)

values of intramolecular hydrogen bond length $H_{25}…O_8$ [N_{15}-$H_{44}…O_8$] are 1.98Å and 2.01Å respectively, that the difference of the theoretical value from the experimental is very low (about 0.03Å) and suggesting the intramolecular hydrogen bond N_{15}-$H_{44}…O_8$ is very strong.

Atomic charge and NMR parameters

We calculated the charge distributions for equilibrium geometry of molecules **I** and **II** by NBO method (natural charge) [25,26] using B3LYP/6-311+G* level. (Atoms labeling is according to Figure 1). The total charge of the investigated molecules is equalto zero. According to Table 3, the calculated results reveal the natural charges for H_{24}, H_{32}, H_{33} and H_{34} atoms in structure **I** are positive value (0.249e, 0.454e, 0.186e and 0.187e, respectively). Therefore the highest positive charge is observed for H_{32} atom due to participate in forming three-centered intramolecular hydrogen bonding ($O_{19}…H_{32}…O_8$). Also H_{24} atom participates in intramolecular hydrogen bonding with O_{17} [C_4-$H_{24}…O_{17}$]. Therefore the charge value of H_{24} atom is the most positive rather than H_{33} and H_{34} atoms. The highest values of negative charge is observed for N_{15} atom (-0.607e). Also O_8, O_{17}, O_{19} and O_{20} atoms have high negative charge (-0.580e, -0.577e, -0.588e and -0.524e, respectively). The C_{18} atom has the most positive charge (0.734) that is due to link to electronegative O_{19} and O_{20} atoms. From calculated natural charge (NBO) is obtained for structure **II**, we found the highest values of negative charges are observed for N_{15} and N_{19} atoms, -0.617e and 0.622e, respectively. Also O_8, O_{18}, O_{27} and O_{34} atoms in structure **II** have high negative charge (-0.580e, -0.593e, -0.580e and -0.574e, respectively). The calculated natural charges for H_{44} and H_{45} atoms in structure **II** are high positive values (0.437e and 0.438e, respectively) that due to participate in forming three-centered intramolecular hydrogen bonding such as $O_8…H_{44}…O_{34}$ and $O_{18}…H_{45}…O_{27}$.

The NMR parameters such as chemical shift isotropic (CS^I) and chemical shift anisotropic (CS^A) for the molecules **I** and **II** are summarized in Table 3. In structure **I**, the CS^I values for H_{24}, H_{32}, H_{33} and H_{34} atoms is 23.031, 20.416, 28.102 and 28.072 ppm, respectively. As seen, H_{32} atom has the lowest CS^I value (20.416 ppm) and highest CS^A value (10.774 ppm), therefore H_{32} atom is the deshielder than other hydrogen atoms that it is as a result of forming three-centered intramolecular hydrogen bond [$O_{19}…H_{32}…O_8$]. Also

according to Table 1, in structure **II**, the CS^I values for H_{37}, H_{44}, H_{45} and H_{46} atoms is 25.354, 22.659, 22.298 and 23.620 ppm, respectively. As seen, H_{44} and H_{45} atoms have the lowest CS^I value (22.659 and 22.298 ppm, respectively) and highest CS^A value (13.276 and 11.868 ppm, respectively), therefore H_{44} and H_{45} atoms are the deshielder than other H_{37} and H_{46} atoms that it is as a result of forming three-centered intramolecular hydrogen bond [O_8…H_{44}…O_{34} and O_{18}…H_{45}…O_{27}].

Electronic properties

Quantum chemical methods are important to obtain information about molecular structure and electrochemical behavior. The Frontier Molecular Orbitals (FMO) analysis calculated for compounds using B3LYP/6-311+G* level [26]. The results

Table 3. The Natural Charge (NBO charges, e) and NMR parameters (ppm) such as chemical shift isotropic (CS^I) and chemical shift anisotropic (CS^A) for compounds **I** and **II** using B3LYP/6-311+G*level

	Natural Charge	**CS^I (ppm)**	**CS^A (ppm)**
Compound I			
C_2	-0.169	54.297	185.975
C_3	0.204	34.439	155.239
O_8	-0.580	-276.578	921.097
N_{15}	-0.607	110.860	152.232
C_{16}	0.591	24.480	78.626
O_{17}	-0.577	-93.434	669.744
C_{18}	0.734	16.450	75.482
O_{19}	-0.588	-72.104	586.068
O_{20}	-0.524	106.128	145.793
H_{24}	0.249	23.031	10.072
H_{32}	0.454	20.416	10.774
H_{33}	0.186	28.102	5.122
H_{34}	0.187	28.072	5.220
Compound II			
C_4	0.224	36.200	154.519
C_7	0.555	-21.591	156.889
O_8	-0.580	-279.263	925.461
N_{15}	-0.617	106.531	111.484
C_{16}	0.618	12.503	109.486
C_{17}	0.614	13.730	101.805
O_{18}	-0.593	-114.191	622.729
N_{19}	-0.622	105.804	122.701
O_{27}	-0.580	-277.384	930.478
O_{34}	-0.574	-113.389	599.195
H_{37}	0.212	25.354	5.377
H_{44}	0.437	22.659	13.276
H_{45}	0.438	22.298	11.868
H_{46}	0.249	23.620	8.357

of FMO such as E_{HOMO}, E_{HOMO-1}, E_{LUMO}, E_{LUMO+1} and HOMO-LUMO energy gap (Eg) of molecules **I** and **II** are summarized in Table 7. The values of energy of the lowest unoccupied molecular orbital (LUMO) and the highest occupied molecular orbital (HOMO) [27]. The HOMO can act as an electron donor and the LUMO can act as the electron acceptor. A higher E_{HOMO} for the molecule indicates a higher electron-donating ability to an appropriate acceptor molecule with a low-energy empty molecular orbital [28]. As seen in Figure 6(a) charge transfer is taking place within molecules **I** and **II**. The graphic pictures of HOMO and LUMO orbitals show HOMO orbital of structure **I** is localized mainly on one of the phenyl rings and amid functional group, while LUMO orbital is focused mainly on phenyl rings, amid functional group and carbonyl group. The HOMO→LUMO transition implies an electron density transfer from one phenyl ring to another phenyl ring. The HOMO orbital of structure **II** is localized mainly on the two middle rings and two amid functional groups, whereas LUMO orbital is focused mainly on the two outer phenyl rings and two carbonyl groups.

Also in this work, electronic structure of compounds **I** and **II** was studied using total densities of states (DOSs) [29,30]. DOS plot shows population analysis per orbital and demonstrates a simple view of the character of the molecular orbitals in a certain energy range [31]. According to Figure 6(b), DOS analysis indicates calculated energy gaps (Eg) for molecules **I** and **II**. A large energy gap implies high stability for the molecule. According to Table 1, HOMO–LUMO energy gap (Eg) value of structure **I** (4.24 eV) is higher than of structure **II** (4.20 eV). Therefore structure **I** is less reactive rather than structures **II**.

A detail of quantum molecular descriptors of structures **I** and **II** are summarized in Table 7. The *I* is Ionization potential ($I = -E_{HOMO}$) and *A* is Ionization potential and Electron affinity ($A = -E_{LUMO}$) [26]. The Chemical hardness ($\eta = (I - A)/2$) is important property to measure the molecular stability and reactivity [32]. A hard molecule has a large energy gap (Eg) and a soft molecule has a small energy gap (Eg) [33]. The Chemical hardness (η) values of structures **I** and **II** are 2.12 and 2.1 eV respectively, therefore structure **I** is a hard molecule and less reactive with high energy gap (Eg = 4.24 eV) rather than structure **II** (Eg = 4.19 eV). The electronic chemical potential ($\mu = -(I + A)/2$) is a form of the potential energy [The absorbed or released energy during a chemical reaction or change during a phase transition] [34]. The μ value of structure **II** is the most negative value (-4.59 eV) rather than structure **I** (-4.52 eV). The electrophilicity parameter (ω) show the stabilization in energy when the system acquires an additional electronic charge from the environment. The electrophilicity index ($\omega = \mu^2/2\eta$) contains information about both electron transfer (chemical potential) and stability (hardness) and is a better descriptor of global chemical reactivity [35]. The higher the value of electrophilicity index displays the high capacity of the molecule to accept electrons. The electrophilicity index for structures **I** and **II** is 4.82 and 5.02 eV, respectively. The structure **II** has the highest electrophilicity index, therefore it has high capacity for acceptance electrons. Dipole moment (μ_D) is a good measure for the asymmetric nature of a structure [26]. The size of the dipole moment depends onthe composition and dimensionality of the 3D structures. As shown in Table 7, the dipole moment of structures **I** and **II** is 2.541 and 7.069 Debye. Therefore structure **II** has the highest value of dipole moment (7.069 Debye) which refers high

asymmetry in the structure and irregularly arranged which gives rise to the increased dipole moment.

Table 4. Molecular properties of compounds **I** and **II** calculated using DFT (B3LYP/6-311+G*)

	E_{HOMO}	E_{LUMO}	E_{HOMO-1}	E_{LUMO+1}	Eg	I	A	μ	η	ω	μ_D	*Point Group*
I	-6.64	-2.4	-7.15	-1.72	4.24	6.64	2.4	-4.52	2.12	4.82	2.541	C1
II	-6.69	-2.49	-6.79	-2.36	4.20	6.69	2.49	-4.59	2.1	5.02	7.069	C1

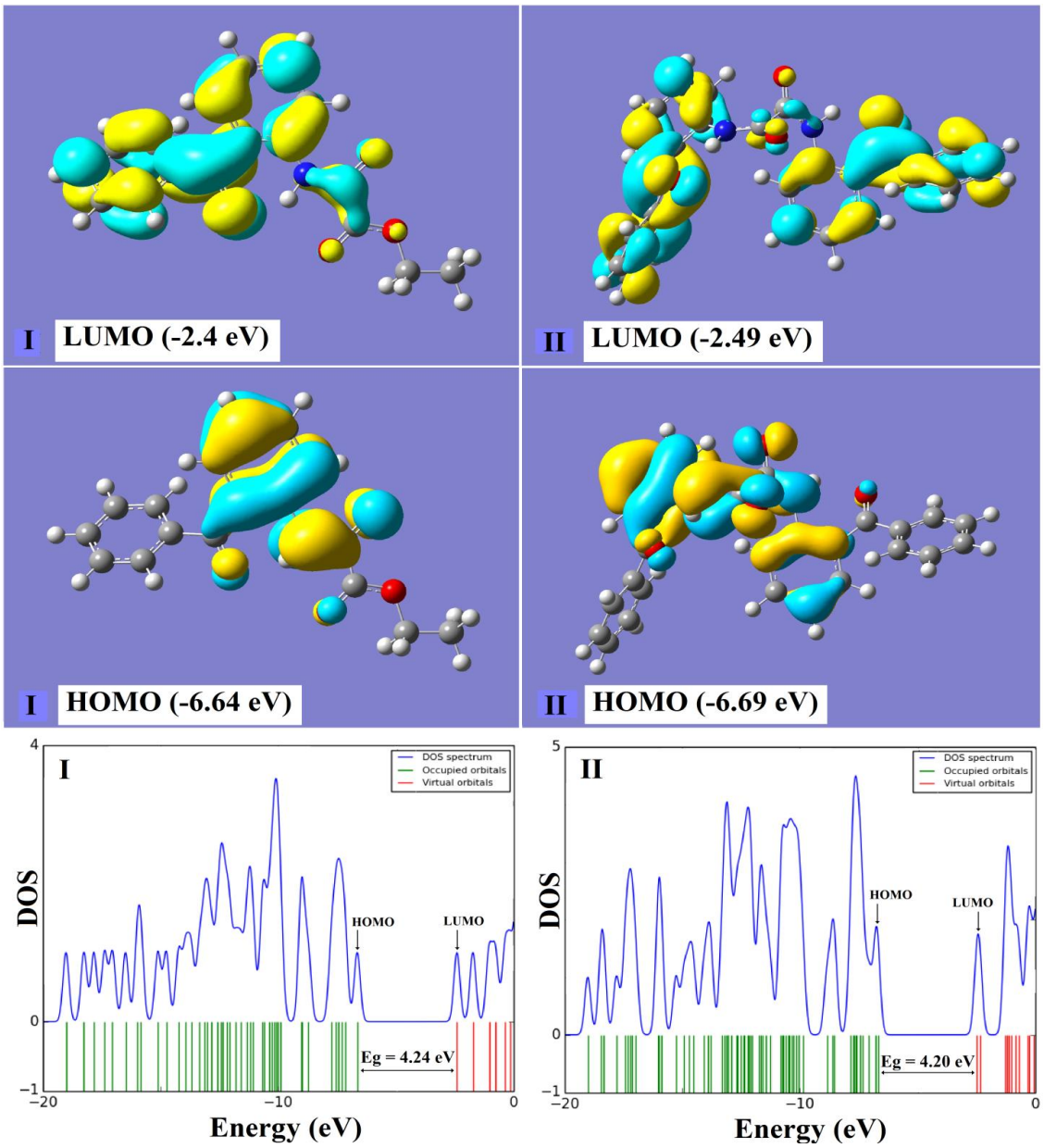

Fig. 2. Calculated Frontier molecular orbitals of structures **I** and **II** (ΔE:energy gap between LUMO and HOMO), (b): Calculated DOS plots of structures **I** and **II** (usingB3LYP/6-311+G*).

Molecular electrostatic potential (MEP)

The molecular electrostatic potential (MEP) was checked out by theoretical calculations using B3LYP/6-311+G* level. Molecular electrostatic potential shows the electronic density and is useful in recognition sites for electrophilic attack and nucleophilic reactions as well as hydrogen bonding interactions [36,37]. The negative areas (red color) of MEP were related to electrophilic reactivity and the positive areas (blue color) ones to nucleophilic reactivity shown in Figure 7. Molecular electrostatic potential V(r) [38] values are $-7.664e^{-2}$ for **I** and $-8.370e^{2}$ for **II**. According to the MEP maps in Figure 7, negative region of compound **I** is mainly focused on O_8, O_{17} and O_{19} atoms with more color intensity (carbonyl groups). Therefore there are three positions on compound **I** for electrophilic attack. As shown in MEP map of the molecule **II**, the negative site is mainly focused on the O_{18} and O_{34} atoms (carbonyl groups). In structures **I** and **II**, hydrogen atoms of N-H groups are not suitable site for nucleophilic activity (not blue color) that it is due to the fact that hydrogen atoms of N-H groups participate in the formation of intramolecular hydrogen bonding.

Thermodynamic Analysis

The relative energy (ΔE), standard enthalpies (ΔH), entropies (ΔS), Gibbs free energy (ΔG) and constant volume molar heat capacity (Cv) values of structures **I** and **II** were obtained by theoretical calculated using the B3LYP/6-311+G* level. Thermodynamic calculations indicates that the relative energies (ΔE), enthalpies (ΔH) and Gibbs free energy (ΔG) for compounds **I** and **II** are negative values while the calculated entropies (ΔS) are positive that indicate three molecules are stable in the gas phase (see Table 5). Also we found that the structure **II** has greater stability rather than structure **I** that due to existence six intramolecular hydrogen bondings in structure **II**, whereas structure **I** has three intramolecular hydrogen bonding.

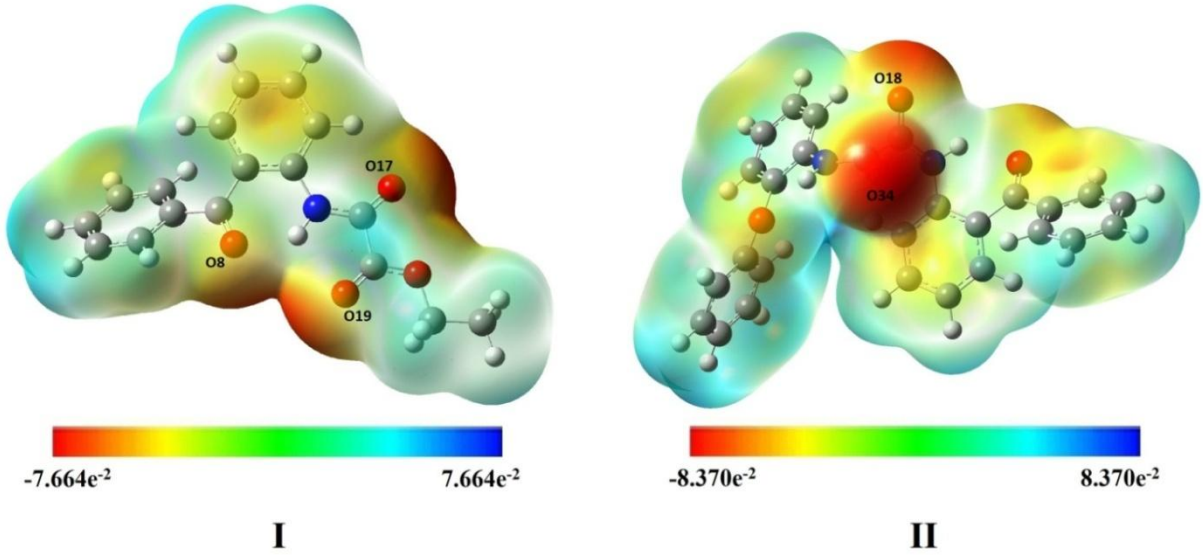

Fig. 3. Molecular electrostatic potential (MEP) maps of structures **I** and **II** calculated using B3LYP/6-311+G* level.

Table 5. Relative thermochemical parameters of structures **I** and **II** calculated using B3LYP/6-311+G* level

Compound	ΔE(Kcal/mol)	ΔG(Kcal/mol)	ΔH(Kcal/mol)	ΔS(cal/molK)	Cv(cal/molK)
I	-635333.3424	-635377.7607	-635332.7500	150.967	73.249
II	-934592.8815	-934650.1737	-934592.2891	194.147	108.536

NBO analysis

Natural bond orbital (NBO) analysis is important method for studying intra- and inter-molecular bonding and interaction between bonds [39,40]. The results of NBO analysis such as the occupation numbers with their energies for the interacting NBOs and the polarization coefficient amounts of atoms for structures **I** and **II** are presented using B3LYP/6-311+G* level is summarized in Table 6. The size of polarization coefficients shows the importance of the two hybrids in the formation of the bond. According to Table 6, in structure **I**, the bonding orbital of the C_3-N_{15} is BD(1) = $0.6201sp^{2.67}+0.7845sp^{1.75}$ and the N_{15}-C_{16} is BD(1)= $0.7915sp^{1.84}+0.6112sp^{2}$. The polarization coefficients of two bonds C_3-N_{15} and N_{15}-C_{16} is shown importance of N_{15} atom in forming these two bonds. Also the natural charge (NBO) of N_{15} atom is more negative value (-0.607e) while C_3 and C_{16} atoms are positive values (0.204e and 0.591e, respectively). Therefore more charge density resides on N_{15} and is electron-rich. According to the calculated bonding orbitals for the C_7-O_8, C_{16}-O_{17}, C_{18}-O_{19} and C_{18}-O_{20}, the polarization coefficients of oxygen atoms are greater than carbon atoms that it is shown importance of O_8, O_{17}, O_{19} and O_{20} in forming C_7-O_8, C_{16}-O_{17}, C_{18}-O_{19} and C_{18}-O_{20} bonds rather than C_7, C_{16} and C_{18} atoms. The calculated bonding orbital for the C_2-C_7 is BD(1) = $0.7200sp^{2.24}+0.6940sp^{1.83}$ with occupancy 1.97626a.u. and energy -0.67235a.u.. The polarization coefficient of C_2 (0.7200) is greater than C_7 (0.6940) that it shown importance of C_2 atom in forming bond C_2-C_7 rather than C_7 atom. Also natural charge of C_2 atom is negative value (-0.169e) and C_7 atom positive value (0.548e). Therefore more charge density is focused on C_2 and is electron-rich. In structure **II**, the calculated bonding orbital for the C_7-O_8 bond is the BD(1)= $0.5895sp^{2.35}d^{0.01}+0.8078sp^{1.40}$ with high occupancy 1.99230a.u. and low energy -1.07618a.u.. The polarization coefficients of C_7= 0.5895 and O_8= 0.8078 are shown importance of O_8 atom in forming these bond and suggest that O_8 atom is more electron rich than the C_7 atom. The calculated natural charge (NBO) of O_8 atom is more negative (-0.580e) rather than C_7 atom (0.555e). Thus more the charge density resides on the O_8 atom. Also the polarization coefficients of other C-O bonds are shown importance of oxygen atom in forming these bonds. Also in the bonding orbital of the C_4-N_{15} [BD(1)= $0.6204sp^{2.80}d^{0.01}+0.7843sp^{1.73}$] with high occupancy 1.98387a.u. and low energy -0.81031a.u., the polarization coefficient of C_4(0.6204) is greater than N_{15}(0.7843) that this suggest N_{15} is more electron-rich (-0.617e) rather than C_4(0.224e). The bonding orbital of the C_{16}-C_{17} is BD(1)= $0.7071sp^{1.97}+ 0.7072sp^{1.97}$. These polarization coefficients C_{16}(0.7071) and C_{17}(0.7072) shows importance both hybrids almost the same in the formation of the bond of C_{16}-C_{17} bond. The calculated natural charges (NBO) of C_{16} and C_{17} atoms are positive values (0.618e and 0.614e, respectively).

Table 6. Calculated natural bond orbitals (NBO) and the polarization coefficient for each hybrid in selected bonds of compounds **I** and **II** using B3LYP/6-311+G* level

Energy (a.u.)	Bond (A-B)[a]	Occupancy (a.u.)	A	B
Compound I				
-0.70559	BD (1) C_2-C_3	1.96909	0.7072 $sp^{1.95}$	0.7070 $sp^{1.80}$
-0.67235	BD (1) C_2-C_7	1.97626	0.7200 $sp^{2.24}$	0.6940 $sp^{1.83}$
-0.65820	BD (1) C_{16}-C_{18}	1.97172	0.7059 $sp^{2.11}$	0.7083 $sp^{1.84}$
-0.64558	BD (1) C_{21}-C_{22}	1.99177	0.7132 $sp^{2.19}$	0.7009 $sp^{2.45}$
-0.81789	BD (1) C_3-N_{15}	1.98629	0.6201 $sp^{2.67}$	0.7845 $sp^{1.75}$
-1.07311	BD (1) C_7-O_8	1.99252	0.5898 $sp^{2.36}d^{0.01}$	0.8076 $sp^{1.41}$
-1.08506	BD (1) C_{16}-O_{17}	1.99399	0.5984 $sp^{1.89}$	0.8012 $sp^{1.46}$
-1.10569	BD (1) C_{18}-O_{19}	1.99601	0.5929 $sp^{1.84}$	0.8053 $sp^{1.48}$
-0.95932	BD (1) C_{18}-O_{20}	1.99225	0.5634 $sp^{2.36}d^{0.01}$	0.8262 $sp^{2.03}$
-0.84621	BD (1) N_{15}-C_{16}	1.98839	0.7915 $sp^{1.84}$	0.6112 sp^{2}
Compound II				
-0.81031	BD (1) C_4-N_{15}	1.98387	0.6204 $sp^{2.80}d^{0.01}$	0.7843 $sp^{1.73}$
-1.07618	BD (1) C_7-O_8	1.99230	0.5895 $sp^{2.35}d^{0.01}$	0.8078 $sp^{1.40}$
-0.84725	BD (1) N_{15}-C_{16}	1.98835	0.7907 $sp^{1.78}$	0.6122 $sp^{2.04}$
-0.66412	BD (1) C_{16}-C_{17}	1.97490	0.7071 $sp^{1.97}$	0.7072 $sp^{1.97}$
-1.01239	BD (1) C_{16}-O_{18}	1.99167	0.5943 $sp^{2.21}d^{0.01}$	0.8042 $sp^{1.76}$
-1.04106	BD (1) C_{17}-O_{34}	1.99094	0.5955 $sp^{2.14}d^{0.01}$	0.8033 $sp^{1.62}$
-0.81447	BD (1) N_{19}-C_{20}	1.98595	0.7839 $sp^{1.71}$	0.6209 $sp^{2.70}$
-1.08020	BD (1) C_{26}-O_{27}	1.99233	0.5895 $sp^{2.36}d^{0.01}$	0.8077 $sp^{1.40}$

[a] A-B is the bond between atom A and atom B. (A: natural bond orbital and the polarization coefficient of atom; A-B: natural bond orbital and the polarization coefficient of atom B).

Electron donor orbital, acceptor orbital and the interacting stabilization energy resulting from the second-order micro disturbance theory [41] are reported in Table 7. The electron delocalization from filled NBOs (donors) to the empty NBOs (acceptors) describes a conjugative electron transfer process between them [42]. For each donor (*i*) and acceptor (*j*), the stabilization energy *E*(2) associated with the delocalization *i*→*j* is estimated. The resonance energy (E(2)) detected the quantity of participation of electrons in the resonance between atoms.[15] The results of the NBO analysis, such as resonance energy (E(2)), donor NBO (i) and acceptor NBO (j), for compound **I** and **II** using B3LYP/6-311+G* level are listed in Table 7. From results of the NBO analysis for compound **I**, the resonance energies (E(2)) of for LP(1)O_8→BD*(1)N_{15}-H_{32} and LP(2)O_8→BD*(1)N_{15}-H_{32} is 2.58 and 5.83 kcal/mol, respectively. These results suggest existence a intramolecular hydrogen bond of O_8…H_{32}-N_{15}. The calculated natural charge of O_8 (–0.580e) and H_{32} (0.454e) that are taking part in intramolecular charge transfer is indicated in the NBO analysis. Also LP(2)O_{19} participates as donor and the anti-bonding BD*(1)N_{15}-H_{32} orbital act as acceptor and their resonance energies (E(2)) is 1.41 kcal/mol that indicate charge transfer from the bonding orbital LP(2)O_{19} to the anti-bonding orbital BD*(1)N_{15}-H_{32} that is shown existence a intramolecular hydrogen bond of O_{19}…H_{32}-N_{15}. These results suggest forming three-centered intramolecular hydrogen bond O_8…H_{32}…O_{19}. In compound **I**, LP(1)N_{15} orbital participates as donor and the anti-bonding BD*(2)C_2-C_3 and BD*(2)C_{16}-O_{17} orbitals act as acceptor and their resonance energies (E(2)) is 37.94 and 62.57 kcal/mol respectively, that shown large charge transfer from the LP(1)N_{15} to the anti-

bonding orbital of BD*(2)C_{16}-O_{17} [LP(1)N_{15}→BD*(2)C_{16}-O_{17}] rather than BD*(2)C_2-C_3 orbital. As shown in Table 7, the resonance energies (E(2)) of LP(1)O_{17}→BD*(1)C_4-H_{24} and LP(2)O_{17}→BD*(1)C_4-H_{24} is 0.61 and 1.22 kcal/mol respectively, that shown existence interaction of O_{17}…H_{24}-C_4. The LP(2)O_{20} orbital participates as donor and the anti-bonding BD*(2)C_{18}-O_{19}, BD*(1)C_{21}-H_{33} and BD*(1)C_{21}-H_{34} orbitals act as acceptor and their resonance energies (E(2)) is 53.18, 4.31 and 4.25 kcal/mol, respectively. These values indicate large charge transfer from the LP(2)O_{20} to anti-bonding orbital of BD*(2)C_{18}-O_{19} [LP(1)N_8→BD*(1)C_7-H_{25}]. According to the results of the NBO analysis for compound **II**, the resonance energies (E(2)) for LP(1)O_8→BD*(1)N_{15}-H_{44} and LP(2)O_8→BD*(1)N_{15}-H_{44} is 1.45, and 3.23 kcal/mol respectively, that suggest existence intramolecular hydrogen bond of O_8…H_{44}-N_{15}. As shown in Table 7, the resonance energies (E(2)) of LP(1)N_{19}→BD*(2)C_{17}-O_{34} and LP(1)N_{19}→BD*(2)C_{20}-C_{21} is 50.11 and 25.63 kcal/mol, respectively. These values indicate large charge transfer from the LP(1)N_{19} to anti-bonding orbital of BD*(2)C_{17}-O_{34} [N_{19}→C_{17}-O_{34}]. Also the resonance energies (E(2)) of LP(1)O_{27}→BD*(1)N_{19}-H_{45} and LP(2)O_{27}→BD*(1)N_{19}-H_{45} is 1.78 and 4.19 kcal/mol respectively, that shown existence intramolecular hydrogen bond of O_{27}…H_{45}-N_{19}. The calculated natural charge of O_{27} (–0.580e) and H_{45} (0.438e) that are taking part in intramolecular charge transfer is indicated in the NBO analysis.

Table 7. Significant donor–acceptor interactions and second order perturbation energies of compounds **I** and **II** calculated using B3LYP/6-311+G* level

Donor NBO(i)	Acceptor NBO(j)	E(2) [a] (kcal/mol)	E(j)-E(i) [b] (a.u.)	F(i , j) [c] (a.u.)
Compound I				
LP (1) O_8	BD*(1) N_{15}-H_{32}	2.58	1.11	0.048
LP (2) O_8	BD*(1) N_{15}-H_{32}	5.83	0.69	0.058
LP (1) N_{15}	BD*(2) C_2-C_3	37.94	0.28	0.093
	BD*(2) C_{16}-O_{17}	62.57	0.27	0.119
LP (1) O_{17}	BD*(1) C_4-H_{24}	0.61	1.15	0.024
LP (2) O_{17}	BD*(1) C_4-H_{24}	1.22	0.72	0.027
LP (2) O_{19}	BD*(1) N_{15}-H_{32}	1.41	0.69	0.029
LP (2) O_{20}	BD*(2) C_{18}-O_{19}	53.18	0.33	0.118
	BD*(1) C_{21}-H_{33}	4.31	0.71	0.052
	BD*(1) C_{21}-H_{34}	4.25	0.71	0.052
Compound II				
LP (1) O_8	BD*(1) N_{15}-H_{44}	1.45	1.10	0.036
LP (2) O_8	BD*(1) N_{15}-H_{44}	3.23	0.68	0.043
LP (1) N_{15}	BD*(1) C_3-C_4	2.62	0.77	0.044
	BD*(2) C_3-C_4	25.64	0.28	0.77
	BD*(1) C_4-C_5	2.10	0.81	0.040
	BD*(1) C_{16}-O_{18}	1.93	0.82	0.39
	BD*(2) C_{16}-O_{18}	43.32	0.33	0.109
LP (1) O_{18}	BD*(1) C_{21}-H_{46}	0.80	1.15	0.036
LP (2) O_{18}	BD*(1) C_{21}-H_{46}	0.73	0.71	0.021
LP (1) N_{19}	BD*(1) C_{17}-O_{34}	0.71	0.85	0.024
	BD*(2) C_{17}-O_{34}	50.11	0.30	0.113
	BD*(1) C_{20}-C_{21}	1.83	0.82	0.038

Continued Table 7

	BD*(2) C_{20}-C_{21}	25.63	0.28	0.076
	BD*(1) C_{20}-C_{25}	2.55	0.79	0.044
LP (1) O_{27}	BD*(1) N_{19}-H_{45}	1.78	1.10	0.040
LP (2) O_{27}	BD*(1) N_{19}-H_{45}	4.19	0.68	0.049

[a] E(2) means energy of hyperconjucative interactions.
[b] Energy difference between donor and acceptor i and j NBO orbitals.
[c] F(i, j) is the Fock matrix element between i and j NBO orbitals.

CONCLUSION

In the present study, the quantum theoretical calculations two crystal structures of *N*-(2-benzoyl-phenyl) oxalyl consists of three-centered intramolecular hydrogen bonding were performed using density functional theory method (DFT/B3LYP/6-311+G*). In structure **I**, the highest positive charge is observed for H_{32} atom due to participate in forming three-centered intramolecular hydrogen bonding (O_{19}…H_{32}…O_8) and in structure **II**, the H_{44} and H_{45} atoms have high positive natural charges that due to participate in forming three-centered intramolecular hydrogen bondings such as O_8…H_{44}…O_{34} and O_{18}…H_{45}…O_{27}. The CS^I value of the H_{32} in structure **I** and H_{44} and H_{45} in structure **II** show these hydrogens are deshielder than other hydrogen atoms as a result of forming three-centered intramolecular hydrogen bond. Thermodynamic analysis indicates that structure **II** has greater stability rather than structure **I** that due to existence six intramolecular hydrogen bondings. According to the results of the NBO analysis for structure **I**, charge transfer $LP(1)O_8 \rightarrow BD^*(1)N_{15}$-$H_{32}$ and $LP(1)O_{27} \rightarrow BD^*(1)N_{15}$-$H_{32}$ suggest forming three-centered intramolecular hydrogen bond O_8…H_{32}…O_{19}. FMO analysis suggests that charge transfer is taking place within the molecules I and II. The energy gap of structure **I** is higher than structure **II**, therefore structure **I** has the lowest reactivity.

ACKNOWLEDGEMENTS

We thank from research council of Young Researchers and Elite Club of Islamic Azad University, Gorgan Branch, Iran, for financial support.

REFERENCES

[1] F. J. MartInez-MartInez, A. Ariza-Castolo, H. Tlahuext and M. Tlahuextl, R. Contreras, *J. Chem. Soc. Perkin Trans 2.* 2 (1993)1481.
[2] Y. A. Ovchinnikov and V. T. Ivanov, *Tetrahedron* 31 (1975) 2177.
[3] E. S. Stevens, N. Sugawara, G. M. Bonora and C. Tionolo, *J. Am. Chem. Soc.* 102 (1980) 7048.
[4] G. P. Dado and S. H. Gellman, *J. Am. Chem. Soc.* 116 (1994) 1054.
[5] IUPAC, *Compendium of Chemical Terminology*, 2nd ed. (the "Gold Book"), 1997.
[6] M. Baron, S. Giorgi-Renault, J. Renault, P. Mailliet, D. Carre and J. Etienne, *Can. J. Chem.* 62 (1984) 526.
[7] C. J. Cramer, in: *Essentials of Computational Chemistry: Theories and Models*, Wiley, Chichester, 2002.
[8] a) D. Avci and Y. Atalay, *Struct. Chem.* 20 (2009) 185. b) R. B. Nazarski, *J. Phys. Org. Chem. 22* (2009) 834.
[9] S. M. Shoaei, A. R. Kazemizadeh and A. Ramazani, *Chin. J. Struct. Chem.* 30 (2011) 568.
[10] H. Hopfl, B. Gomez and R. Martinez-Palou, *J. Mex. Chem. Soc.* 49 (2005)

307.
[11] H. Sahebalzamani, F. Salimi and E. Dornapour, in: *Hindawi Publishing Corporation Journal of Chemistry*. Vol. 2013, Article ID 187974, 5 pages, 2013.
[12] I. Rozas, I. Alkorta and J. Elguero, *J. Phys. Chem. A* 102 (1998) 9925.
[13] A. Lakshmipriyaa, S. R. Chaudharia, A. Shahic, E. Arunanc and N. Suryaprakasha, *Phys. Chem. Chem. Phys.* DOI: 10.1039/C4CP05917D, 2012.
[14] F.J. MartInez-MartInez, I. I. Padilla-Martínez, M. A. Brito, E. D. Geniz, R. C. Rojas, J. B. Saavedra, H. Hopfl, M. Tlahuextl and R. Contreras, *J. Chem. Soc. Perkin Trans 2 2* (1998) 401.
[15] C. Z. Gomez-Castro, I. I. Padilla-Martinez, E. V. Garcia-Baez, J. L. Castrejon-Flores, A. L. Peraza-Campos and F.J. Martinez-Martinez, *Molecules 19* (2014) 14446.
[16] W. Kohn, A. D. Becke and R. G. Parr, *J. Phys. Chem.* 100 (1996) 12974.
[17] M. J. Frisch, G. W. Trucks, H. B. Schlegel, G. E. Scuseria, M. A. Robb., J. R. Cheeseman, J. A. Montgomery, T. Vreven, K. N. Kudin, J. C. Burant, J.M. Millam, S. S. Iyengar, J. Tomasi, V. Barone, B. Mennucci, M. Cossi, G. Scalmani, N. Rega, G. A. Petersson, H. Nakatsuji, M. Hada, M. Ehara, K. Toyota, R. Fukuda, J. Hasegawa, M. Ishida, T. Nakajima, Y. Honda, O. Kitao, H. Nakai, M. Klene, X. Li, J. E. Knox, H. P. Hratchian, J. B. Cross, V. Bakken, C. Adamo, J. Jaramillo, R. Gomperts, R. E. Stratmann, O. Yazyev, A. J. Austin, R. Cammi, C. Pomelli, J.W. Ochterski, P. Y. Ayala, K. Morokuma, G. Voth, P. Salvador, J. J. Dannenberg, V. G. Zakrzewski, S. Dapprich, A. D. Daniels, M. C. Strain, O. Farkas, D. K. Malick, A. D. Rabuck, K. Raghavachari, J. B. Foresman, J. V. Ortiz, Q. Cui, A. G. Baboul, S. Clifford, J. Cioslowski, B. B. Stefanov, G. Liu, A. Liashenko, P. Piskorz, I. Komaromi, R. L. Martin, D. J. Fox, T. Keith, M. A. Al-Laham, C. Y. Peng, A. Nanayakkara, M. Challacombe, P. M. W. Gill, B. Johnson, W. Chen, M. W. Wong, C. Gonzalez and J. A. Pople, *Gaussian 03, revision B03, Gaussian Inc.*, Pittsburgh, PA, 2003.
[18] M. Monajjemi, M. Sheikhi, M. Mahmodi Hashemi, F. Molaamin and R. Zhiani, *Inter. J. Phys. Sci.* 7 (2012) 2010.
[19] L. Shiri, D. Sheikh, A. R. Faraji, M. Sheikhi and S. A. Seyed Katouli, *Lett. Org. Chem.* 11 (2014) 18.
[20] A. R. Soltani, M. T. Baei, M. Mirarab, M. Sheikhi and E. Tazikeh Lemeski, *J. Phys. Chem. Solids* 75 (2014) 1099.
[21] A. Frisch, A. B. Nielson and A. J. Holder, GAUSSVIEW User Manual, Gaussian Inc., Pittsburgh, PA, 2000.
[22] M. Monajjemi, S. Afsharnezhad, M. R. Jaafari, T. Abdolahi, A. Nikosadeand and H. Monajjemi, *Phys. Chem. Liquids* 49 (2011) 318.
[23] H. Tanak, *J. Phys. Chem. A* 115 (2011) 13865.
[24] M. H. Habibi, E. Shojaee, M. Ranjbar, H. R Memarian, A. Kanayama and T. Suzuki, *Spec. Acta. Part A* 105 (2013) 563.
[25] S. Guidara, H. Feki and Y. Abid, *Spectro. Chim. Acta A Mol. Biomol. Spectrosc.* 133 (2014) 856.
[26] M. Sheikhi, D. Sheikh and A. Ramazani, *S. Afr. J. Chem.* 67 (2014) 151.
[27] K. G. Vipin Das, C. Yohannan Panicker, B. Narayana, P. S. Nayak, B. K. Sarojini and A. A. Al-Saadi, *Spectrochim. Acta A Mol. Biomol. Spectrosc.* 135 (2015) 162.
[28] S. Sebastian and N. Sundaraganesan, *Spectrochim. Acta A Mol. Biomol. Spectrosc.* 75 (2010) 941.

[29] F. J. Luque, J. M. Lopez and M. Orozco, *Theor. Chem. Acc.* 103 (2001) 343.
[30] A. Ahmadi Peyghan, M. T. Baei, M. Moghimi and S. Hashemian, *Comput. Theor. Chem.* 997 (2012) 63.
[31] A. Soltani, F. Ghari, A. Dehno Khalaji, E. Tazikeh Lemeski, K. Fejfarova, M. Dusek and M. Shikhi, *Spectrochim. Acta A Mol. Biomol. Spectrosc.* 139 (2015) 271.
[32] R. G. Pearson, *J. Chem. Sci.* 117 (2005) 369.
[33] F. J. Luque, J. M. Lopez and M. Orozco, *Theor. Chem. Acc.* 103 (2000) 343.
[34] T. A. Koopmans, *Physica* 1 (1993) 104.
[35] R. J. Parr, L.V. Szentpaly and S. Liu, *J. Am. Chem. Soc.* 121 (1999) 1922.
[36] N. Okulik and A. H. Jubert, *J. Mol. Des.* 4 (2005) 17-30.
[37] D. Habibi, A. R. Faraji, D. Sheikh, M. Sheikhi and S. Abedi, *RSC Adv.* 4 (2014) 47625.
[38] P. Politzer and P. Lane, *Struct. Chem.* 1 (1990) 159.
[39] F. Weinhold and C. R. Landis, in: Natural Bond Orbitals and Extensions of Localized, 2001.
[40] M. Sheikhi and D. Sheikh, *Rev. Roum. Chim.* 59 (2014) 761.
[41] B. D. Joshi and P. Tandon, S. Jain, *The Himalayan Physics* 3 (2012) 44.
[42] E. D. Glendening, A. E. Reed, J. E. Carpenter and F. Weinhold *NBO version 3.1, TCI*, University of Wisconsin, Madison, 1998.